Available online at www.sciencedirect.com

jmr&t Journal of Materials Research and Technology

journal homepage: www.elsevier.com/locate/jmrt

Original Article

On the fatigue and fracture behavior of keyhole-free friction stir spot welded joints in an aluminum alloy

Guney Guven Yapici [a,b,*], *Isam Jabbar Ibrahim* [a,c]

[a] *Mechanical Engineering Department, Ozyegin University, Istanbul, Turkey*

[b] *Mechanics and Manufacturing of Functional and Structural Materials (MEMFIS) Laboratory, Ozyegin University, Istanbul, Turkey*

[c] *Technical Engineering College, Middle Technical University, Baghdad, Iraq*

ARTICLE INFO

Article history:
Received 6 September 2020
Accepted 3 January 2021
Available online 8 January 2021

Keywords:
Friction stir spot welding
Dissimilar joint
Keyhole
Aluminum
Fatigue
Fracture

ABSTRACT

The target of this research study was to evaluate the shear-tensile and fatigue behavior of aluminum 6061 alloy welds, in two different heat treatment conditions, joined by the recently developed intermediate layer friction stir spot welding (FSSW) technique. The keyhole, which is the disadvantage of the conventional FSSW process, was avoided using an additional intermediate layer (IL) accompanied by a simple tooling. Shear-tensile experiments demonstrated acceptable mechanical performance of IL-FSSW joints in comparison with that obtained using alternative methods. Fatigue behavior of the joints revealed a dependency to pre-processing temper especially at high cyclic load levels with improved life for the aged condition. Observations on the failure regions under shear-tensile experiments exhibited plug type and shear-plug type fracture modes for the aged and annealed conditions, respectively. In contrast, the fracture mode showed variation with respect to the load level but not to the type of temper during cyclic loading.

© 2021 The Authors. Published by Elsevier B.V. This is an open access article under the CC BY-NC-ND license (http://creativecommons.org/licenses/by-nc-nd/4.0/).

1. Introduction

Currently, lightweight materials such as aluminum alloys are extensively used in a variety of structural applications in automotive and aerospace industries. Among different series of aluminum alloys, 6xxx series are highly preferable because of their extrusion capability, corrosion resistance and high strength/weight ratio [1,2]. Among the 6xxx series, AA6061 is considered as one of the most commercially used alloys. However, joining of lightweight metals presents challenges. For instance, although resistance spot welding (RSW) has been extensively used for years in the automotive manufacturing companies, thermal conductivity and electrical conductivity problems make the RSW process unsuitable for joining of lightweight metals due to the large heat distortion and poor weld strength [3]. Additional disadvantages including high operating and maintenance costs limit the application of this method.

* Corresponding author.
E-mail address: guven.yapici@ozyegin.edu.tr (G.G. Yapici).

https://doi.org/10.1016/j.jmrt.2021.01.006

2238-7854/© 2021 The Authors. Published by Elsevier B.V. This is an open access article under the CC BY-NC-ND license (http://creativecommons.org/licenses/by-nc-nd/4.0/).

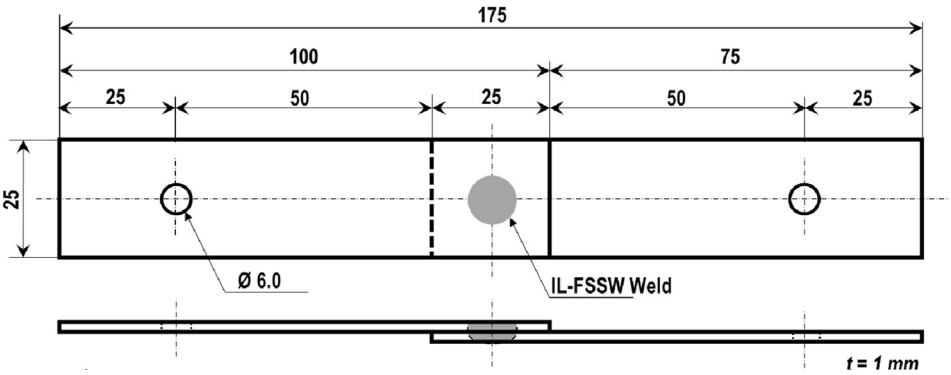


Fig. 1 – Schematic of the mechanical test samples used.

The Welding Institute in Britain developed a linear joining process called friction stir welding (FSW) in 1991 [4,5]. In 1993, based on FSW, Mazda Corporation of Japan proposed a friction stir spot welding (FSSW) process as an alternative to RSW, and applied it to enhance the quality of the hood and rear door production of the RX-8 Mazda sport vehicle [6,7]. As a result, energy consumption was appreciably reduced and cost of the process was decreased by 40%. Since then, FSSW has been considered as a feasible process yielding welded joints with reasonable mechanical properties and free of contamination when compared to RSW or conventional fusion welding processes [8–10].

The FSSW process has been attempted with various modifications such as refill FSSW [11], protrusion FSSW [12], friction spot joining (FSJ) [13,14] or plunge FSSW [15,16], in which a rotating tool is plunged into the overlapping sheets to a prearranged depth before retraction after a dwell period [17,18]. Nevertheless, one of the main disadvantages of the conventional FSSW joints is the keyhole that unavoidably remains at the center of the weld spot. In automotive industry, it is difficult to paint the keyhole region of the joints. Since there can be residual water due to washing, rain or a similar cause in the keyhole, the possibility of corrosion increases and consequently the strength of welded joints decreases [3].

There are only a few studies on the keyhole refilling as a post-treatment following the FSSW process, particularly on the fatigue behavior of these welded joints, which is an important topic for ensuring safe and reliable applications of the welded joints [3,19–22]. For instance, it was reported that the quality of FSSW joints was enhanced using a specially designed tool, which could refill the keyhole [3]. The results showed that tensile strength of the refilled welds improved up to 30% higher than those with the keyhole, while fatigue strength remained nearly the same. Lin et al. [21] detected different failure modes between quasi-static and cyclic loading of Al6061-T6 welded sheets fabricated by FSSW. The same work indicated that under quasi-static loading, upper nugget pull-out failure was prevalent; whereas under fatigue loading, both upper and lower nugget pull-out failures were observed. In addition, a new FSSW process was offered to join AA7075-T6 plates by using a localized plasticity method and enhanced the strength and fatigue life of the welded joints up to six times [22]. However, the keyhole at the center of the weld was converted to an open hole geometry leaving the keyhole problem unsolved.

Most of the previous studies have focused on the fatigue behavior of conventional FSSW welded joints with or without post-treatment for keyhole removal. In the present study, the conventional FSSW technique was improved to avoid the keyhole in-situ using an intermediate layer. In this study, the fracture and fatigue behavior of the 6061 aluminum joints processed using the novel intermediate layer friction stir spot welding (IL-FSSW) technique are evaluated. The effect of initial temper is also probed by focusing on both the annealed (O) and the artificial aged (T6) conditions. The fracture surfaces were examined in detail to support the observations in mechanical response by identifying the responsible failure mechanisms.

2. Experimental procedure

In this study, AA6061 aluminum alloy was supplied from AMAG Metall AG and was used in two different heat treatment conditions of O and T6. Tensile test on the base metal was carried out and the results showed an average tensile strength

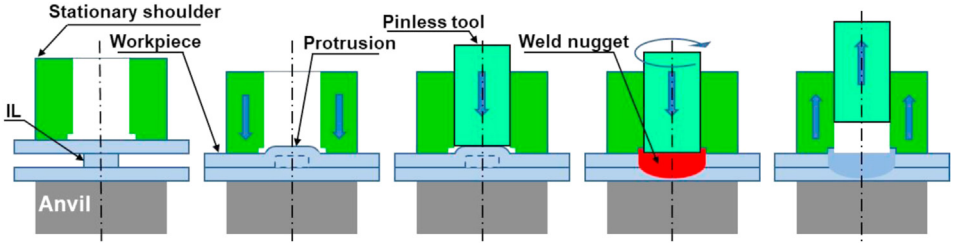


Fig. 2 – Schematic of the IL-FSSW process steps.

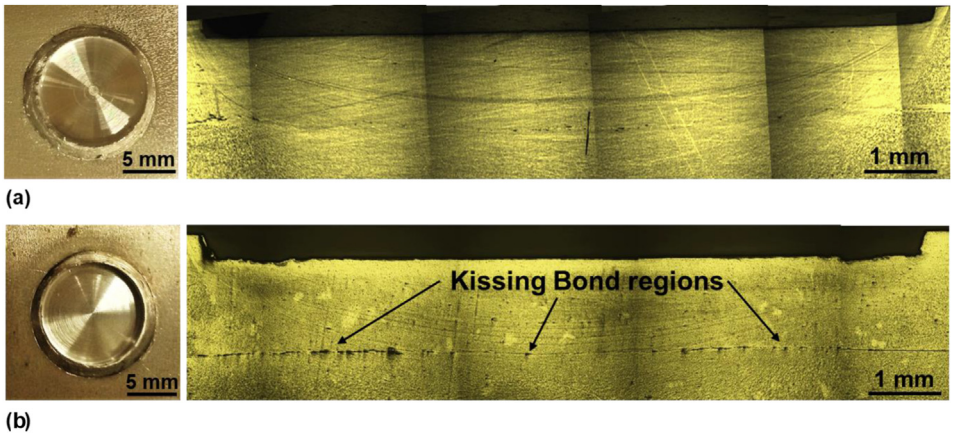


Fig. 3 – Macroscopic appearance of IL-FSSW weld joints, top and cross section view: (a) AA6061-O, (b) AA6061-T6.

of 130.9 and 340.7 MPa for O and T6 condition, respectively. As shown in Fig. 1, the tensile and fatigue specimens were made by using two 25 × 100 mm sheets with a thickness of 1 mm to form welded samples with a 25 × 25 mm overlap area according to the American Welding Society (AWS) standard [23].

Flat spot welds were achieved by a one-step process consisting of a tool with a stationary shoulder and 10 mm diameter flat tip. Additionally, an intermediate layer was used to produce a weld without keyhole as schematically shown in Fig. 2. The workpieces including the intermediate layer (IL) are held in place by the shoulder to form a protrusion in the upper surface of the top sheet over the IL [24–26].

As shown in Fig. 2, the rotationary tool starts moving downward as it plunges into the protrusion at a level higher than the surface of the workpiece. During the plunging process, the frictional heat generated by the rotational tool increases the temperature of the protrusion region on the upper sheet and subsequently that of the IL, which causes softening. The joining process is completed by mixing of the IL with the material of upper sheet and lower sheet due to the stirring action. The tool retracts back leaving a flat spot weld without keyhole formation. The welding parameters used in this study were as follows; i) tool rotational speed of 1200 rpm, ii) plunging feed rate of 20 mm/min, and iii) plunging depth of 0.9 mm.

The samples were cut from the cross-section of the welded zone using electro-discharge machining (EDM) and were prepared according to standard metallographic procedures including grinding, polishing and etching to discern the effect of processing on microstructural development of the samples. The etching solution used for AA6061 was Keller's reagent consisting of 190 ml distilled water, 5 ml HNO_3, 3 ml HCl, and 2 ml HF [27]. Vickers microhardness experiments were conducted with a force of 100 gf for 15 s indentation duration.

For the shear-tensile test, an Instron 8872 mechanical test frame was utilized at a displacement rate of 0.025 mm/s to evaluate the joint strength. Axial fatigue experiments were conducted at a sinusoidal frequency of 15 Hz and at a stress ratio (R) of 0.1. Both shear-tensile and fatigue tests were repeated three times for each sample to ensure repeatability and the standard deviation of the experiments was lower than 5%. The fracture surfaces of the tested samples were examined in a JEOL JSM-6335F scanning electron microscope (SEM) operating at an accelerating voltage of 15 kV.

3. Results and discussion

3.1. *Post-welding microstructure development*

The macroscopic views of the top and cross-section side of the welded joints processed by IL-FSSW for AA6061 in both O and T6 tempers are shown in Fig. 3. The macroscopic observation of welded samples revealed that spot joints without a keyhole were successfully achieved with the utilization of an intermediate layer. However, when compared to the annealed condition, relatively more kissing bond regions were detected at the interface of the T6 sheets, due to the higher flow strength and hardness of the 6061 alloy in this condition [28,29].

The microstructure of different regions of the welded sample which are known as the base material (BM), heat affected zone (HAZ), thermomechanical affected zone (TMAZ), and stir zone (SZ) are demonstrated in Fig. 4 and Fig. 5 for the O and T6 conditions, respectively. It can be realized that the average grain size (AGS) of the SZ for both conditions was smaller than that of the base material and this grain refinement is attributed to the dynamic recrystallization during the stirring process caused by the presence of an effective plastic deformation field leading to heat generation [25,26]. For the O condition, AGS values in BM, HAZ, TMAZ, and SZ were around 22, 28, 14, and 3 μm, respectively; whereas for the T6 condition, AGS values in BM, HAZ, TMAZ, and SZ were around 15, 23, 12, and 4 μm, respectively.

It is manifested in Fig. 3 through Fig. 5 that the joints were successfully manufactured. Upper, lower sheets and IL were mixed properly in the SZ as indicated by the ambiguous interfaces among neighboring zones. Similar shaped boundaries were observed for the IL-FSSW weld regions, as also recognized for the conventional FSSW [30–32]. However, presence of kissing bond defects at the interfaces of the T6 sheets left some regions partially welded within the weld nugget.

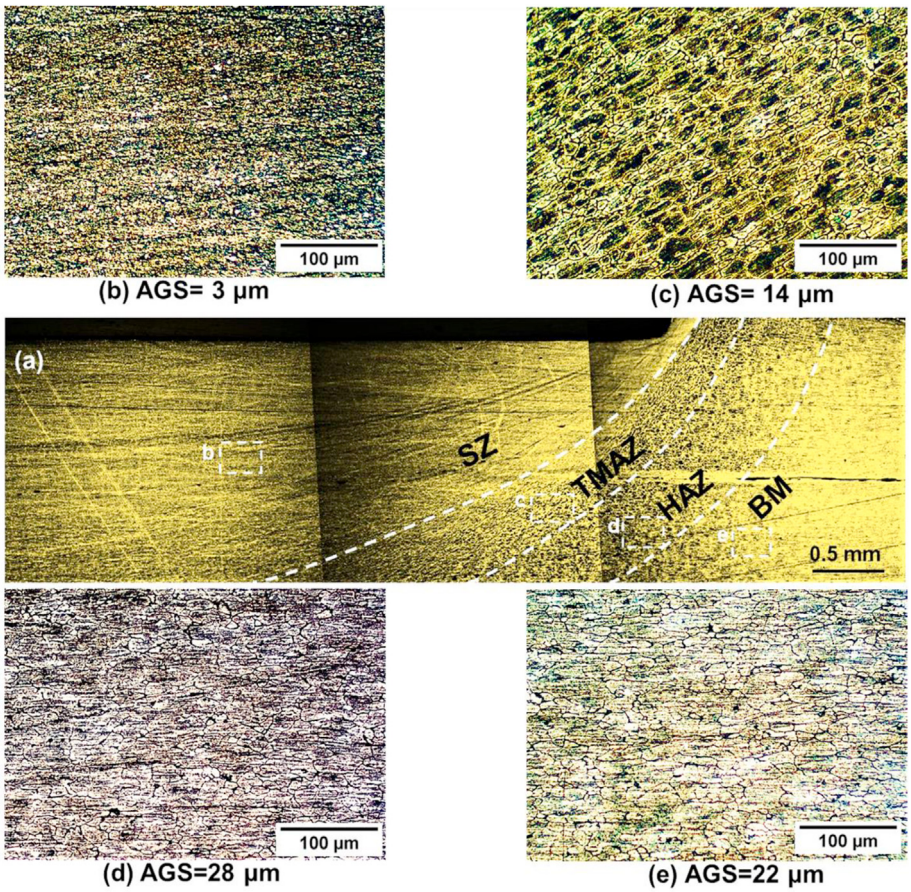


Fig. 4 – (a) Weld regions, average grain size values and microstructures of (b) SZ, (c) HAZ, (d) TMAZ, and (e) BM in IL-FSSW joint for AA6061-O.

3.2. *Post-welding hardness profiles*

Microhardness tests were conducted along four parallel lines on the cross-section, from the center of the welded zone toward the outer edge of the sample. Along each line, measurements were conducted with a spacing of 0.25 mm between each indent as shown in Fig. 6.

As expected, the hardness of AA6061-T6 joint was higher than that of the AA6061-O joint due to the comparably higher pre-weld hardness of the former, as shown in Fig. 6. This explains the lack of appreciable difference in the hardness levels of BM and SZ regions at 1.3 mm level of the AA6061-T6 hardness profile, Fig. 6b. At this depth, the stirring action poorly influenced the microstructure of the T6 condition as compared with that observed for the O temper, Fig. 6a. For the latter (annealed condition), a uniform trend is observed at all levels indicating a homogeneous microstructure throughout the cross-section.

Regardless of the initial temper, the hardness levels at the center of the weld within the SZ are higher than that of the other regions. Far from the center, hardness gradually decreases through the TMAZ towards the HAZ [33]. Outside the HAZ, there is an increasing trend in hardness towards the BM region exhibiting a concave shaped profile. Grain coarsening is probable in the HAZ leading to lower hardness. The SZ is associated with high temperature and severe plastic deformation due to direct contact of the welding tool leading to dynamic recrystallization along with a fine grained structure [19,34].

3.3. *Mechanical behavior under shear-tensile loading*

The mechanical performance of welded joints is characterized by the lap shear failure force (LSFF). The LSFF-displacement curves of the IL-FSSW joints during lap shear testing is shown in Fig. 7. In general, strength properties of friction spot welds should be in minimum on par with the American Welding Society (AWS) standard. The minimum LSFF was calculated according to the AWS recommendations using Eq. (1) as follows [23]:

$$\mathrm{LSFF} = \frac{(-6.36 \times 10^{-7} \times S^2 + 6.58 \times 10^{-4} \times S + 1.674) \times S \times 4 \times t^{1.5}}{1000} \quad (1)$$

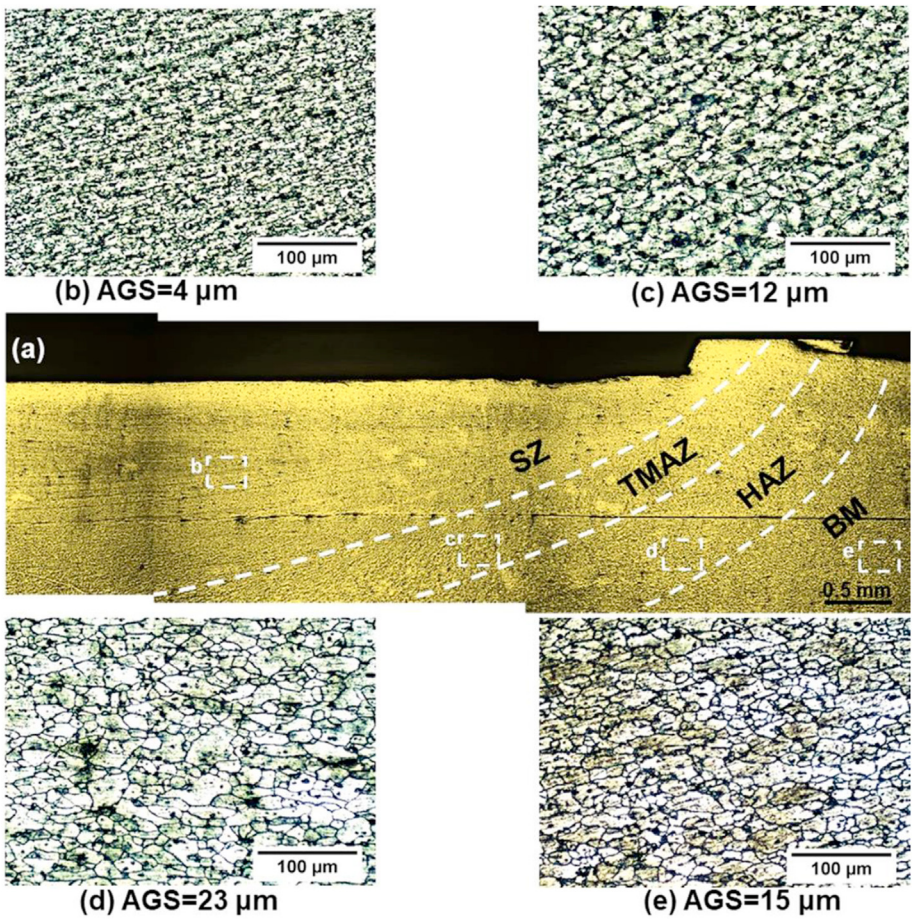


Fig. 5 – (a) Weld regions, average grain size values and microstructures of (b) SZ, (c) HAZ, (d) TMAZ, and (e) BM in IL-FSSW joint for AA6061-T6.

where, S is the ultimate tensile strength of the base metal and t is the sheet thickness. The values of the ultimate tensile strength in Eq. (1) were considered based on the experimental results as 130.9 and 340.7 MPa for AA6061-O and AA6061-T6, respectively. Accordingly, the baseline values of LSFF for the AA6061-O and AA6061-T6 welded samples are 910 and 2480 N, respectively. As shown in Fig. 7, the average LSFF values are 2825.4 and 3261.7 N, which is over 3 and 1.3 times the AWS requirement for the AA6061-O and AA6061-T6 welds, respectively. Thus, it is clear that the joints fabricated by the IL-FSSW process bare appropriate tensile properties as recommended by the AWS.

Moreover, Table 1 demonstrates a comparison of the LSFF and shear strength of welded samples of AA6061 alloy in different heat treatment conditions using various FSSW techniques. The strength of IL-FSSW joints is competitive among the other processes listed in Table 1. Assuming that the weld nugget is dictated by the tool diameter, the respective joint shear stress values are indicated accordingly. Although the joint diameter is not equal to the tool diameter, yet the stress values are provided as a measure of the welded joint strength. Accordingly, strength of the IL-FSSW welds exceed those manufactured by the conventional or alternative FSSW processes [35–39].

The close-up views of the IL-FSSW fractured samples under shear-tensile test are shown in Fig. 8. A combination of mechanisms including sheet tearing and nugget pull out was observed in O condition samples, where failure occurred along the periphery of the spot in the upper sheet at the flash zone traversing through the BM. The upper sheet did not separate fully from the weld zone and the nugget remained in the lower sheet establishing a shear-plug type fracture [3]. In contrast, fracture mode of the welded samples in T6 condition was of plug type. The welds failed along the periphery of the IL, within the TMAZ/HAZ region due to the lower strength in this region, as can be traced from the hardness measurements. Before full fracture, the weld nugget is partially peeled away exposing the interface in between. The reason for this is the presence of kissing bond defects in the interface between the sheets, resulting in partially welded regions in the nugget zone as shown in Fig. 3b.

From the appearance of fracture regions, it can be concluded that better bonding is achieved in O temper joints.

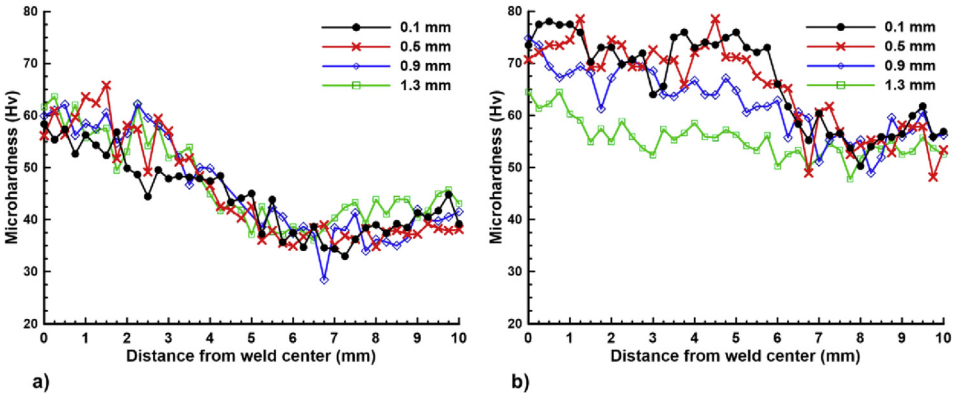


Fig. 6 – Hardness profile of the IL-FSSW sample, tested from the cross-section at four different distances from the top surface: (a) AA6061-O, (b) AA6061-T6.

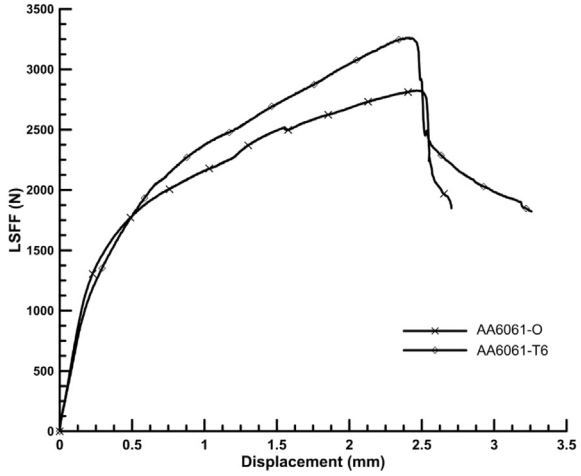


Fig. 7 – Force-displacement curves of the IL-FSSW welded joints.

This is because, unlike the T6 joints there is an evident portion of upper sheet material on the top side of lower sheet. Notwithstanding the temper type, an excellent mixture of the upper sheet and lower sheet with intermediate layer material was observed in the weld nugget.

3.4. *Mechanical behavior under fatigue loading*

The relationship between the maximum load (L_{max}) and the number of cycles to failure (N_f) of AA6061 welds in T6 and O tempers is shown in Fig. 9, as appropriate for the representation of fatigue performance in FSSW lap joints [21,32,40–44]. Although number of cycles to failure for both tempers is almost the same at the lowest load level, the T6 welds have higher fatigue life up to an order of magnitude higher than that of the O welds at increased load levels.

The IL-FSSW joints subjected to seven levels of peak loads (L_{max}) ranging from 500 to 2500 N, where the close-up views of fatigue fracture surfaces at the lowest load level and the highest load level are represented in Fig. 10 and Fig. 11 for both tempers. Regardless of the temper, cracks propagated into the upper sheet at the highest cyclic load and fracture occurred due to crack growth around the nugget zone. Fracture ceases by removal of the nugget which can be denoted as plug type fracture [3].

When the load applied during fatigue is low, crack initiates in the lower sheet as indicated by arrows in Fig. 10d and Fig. 11d, where the crack propagated around the nugget and most of the nugget remained in the lower sheet. Here, fatigue failure originates as crack initiation in the TMAZ and HAZ and propagates along the lower sheet causing it to tear while the

Table 1 – Previous attempts on 6061 alloy welds fabricated by various FSSW processes.

Study	Welding Process	Base Metals Upper Sheet/Lower Sheet	LSFF (kN)	Tool Diameter (mm)	Lap Shear Strength (MPa)
A	FSSW [10], a novel technique	AA6061-T6 (1 mm)/AA6061-T6 (1 mm)	3.77	12	33.4
B	FSSW [35], a novel technique	AA6061-T6 (0.5 mm) IAA6061-T6 (0.5 mm)	1.92	10	24.4
C	Conventional FSSW [36]	AA6061-T6 (3 mm)/AA6061-T6 (3 mm)	3.6	20	11.5
D	FSSW [37], a novel technique	AA6111-T4 (0.93 mm)/AA6111-T4 (0.93 mm)	3.4	10	43.3
E	Conventional FSSW [38,39]	a) AA6061-T6 (2 mm)/AA6061-T6 (2 mm)	2.75	10	35
F	IL-FSSW (the current work)	a) AA6061-O (1 mm)/AA6061-O (1 mm) b) AA6061-T6 (1 mm)/AA6061-T6 (1 mm)	2.83 3.26	10	36.1 41.5

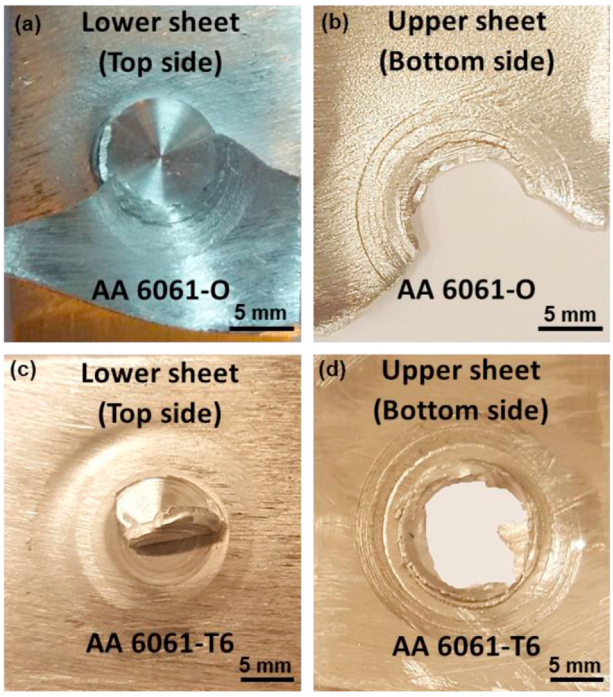


Fig. 8 – The fracture modes after shear-tensile test of joints, the loading direction is vertical: (a) and (b) shear-plug type fracture mode, (c) and (d) plug type fracture mode.

nugget pulls out of the upper sheet. Similar observations were disclosed for the FSSW of 2024 aluminum alloy, where the fracture mode was determined to be of shear-plug type [45]. Finally, the upper and lower sheets were sheared off from each other and got separated.

The discrepancy between the fracture morphologies at different load levels is summarized in Fig. 12. To sum up, fatigue is manifested by crack initiation at the matching surfaces between the upper and lower sheets following the joint line due to stress concentration and crack growth through; (i) the upper sheet under high stress regime to fracture by the plug mode, and (ii) the upper and lower sheets under low stress regime to fracture by the shear-plug mode.

Since fatigue resistance varies mostly for the lowest load level, SEM investigations were carried out on the fracture surface viewing the upper sheet (bottom surface) of the joints. Considering the O welds, Fig. 13b through Fig. 13e represent the magnified views at points B-E in Fig. 13a,

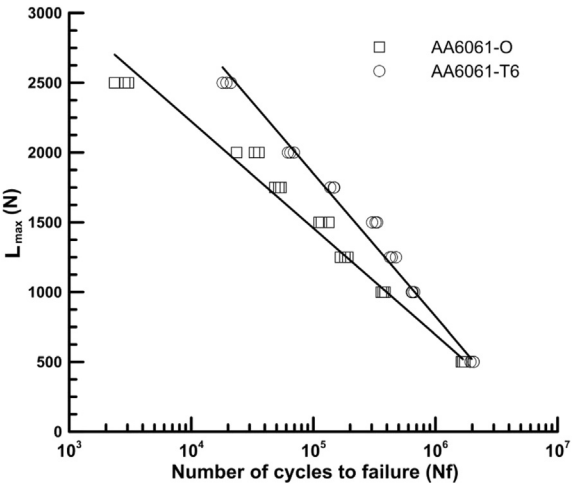


Fig. 9 – Relationship between maximum load and cycles to failure of IL-FSSW joints.

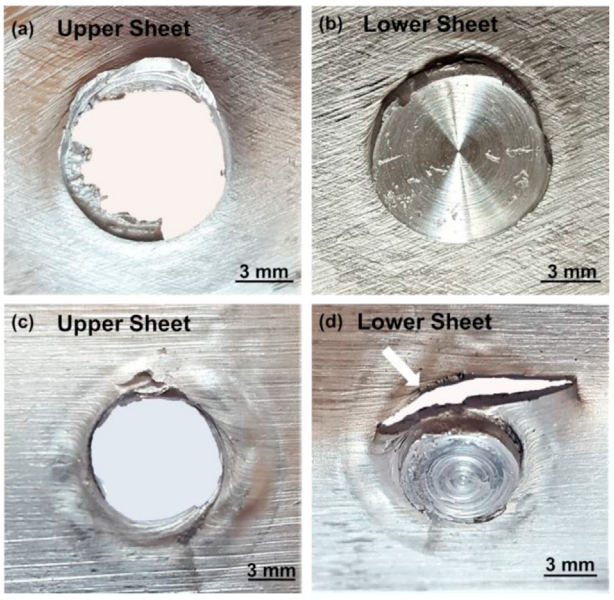


Fig. 10 – Macroscopic appearance of fatigue fractured O temper joints from the upper and lower sheets (bottom and top side), respectively: (a) and (b) L_{max} = 2500 N, (c) and (d) L_{max} = 500 N. The loading direction is vertical.

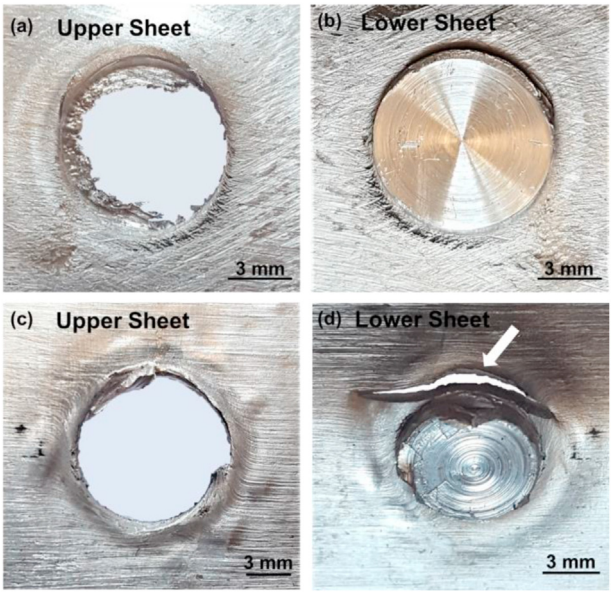


Fig. 11 – Macroscopic appearance of fatigue fractured T6 temper joints from the upper and lower sheets (bottom and top view), respectively: (a) and (b) L_{max} = 2500 N, (c) and (d) L_{max} = 500 N. The loading direction is vertical.

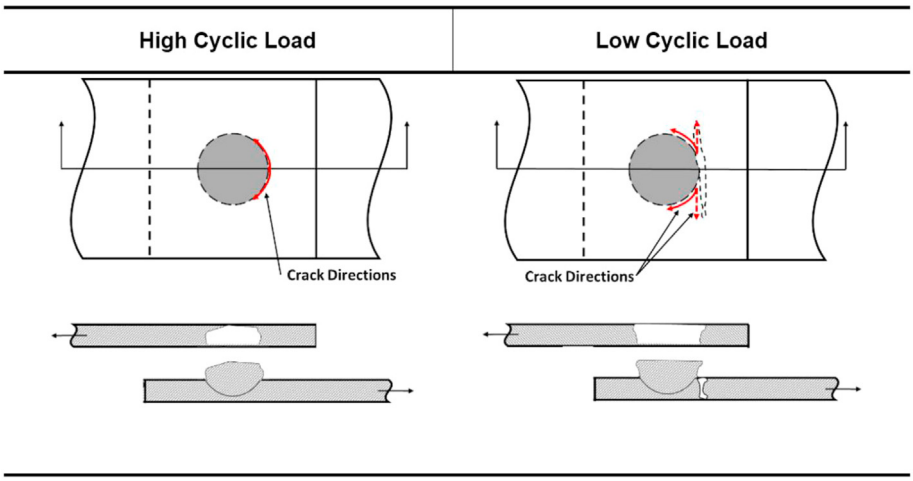


Fig. 12 – Schematic outlining the effect of cyclic load on the fracture morphology.

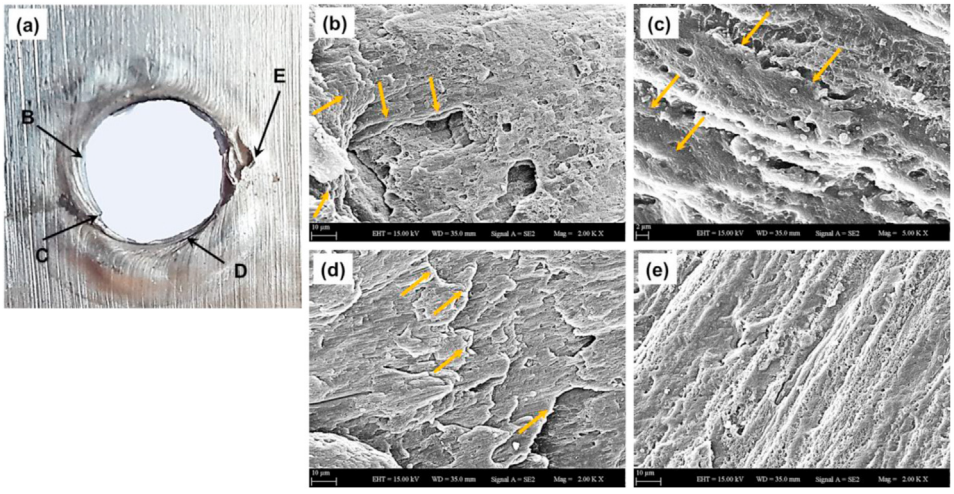


Fig. 13 – Fracture surface images on the upper sheet of O welds, bottom surface: (a) $L_{max} = 500$ N and $N_f = 1.21 \times 10^6$ and (b–e) magnified views at points B-E in (a), respectively. The loading direction is horizontal.

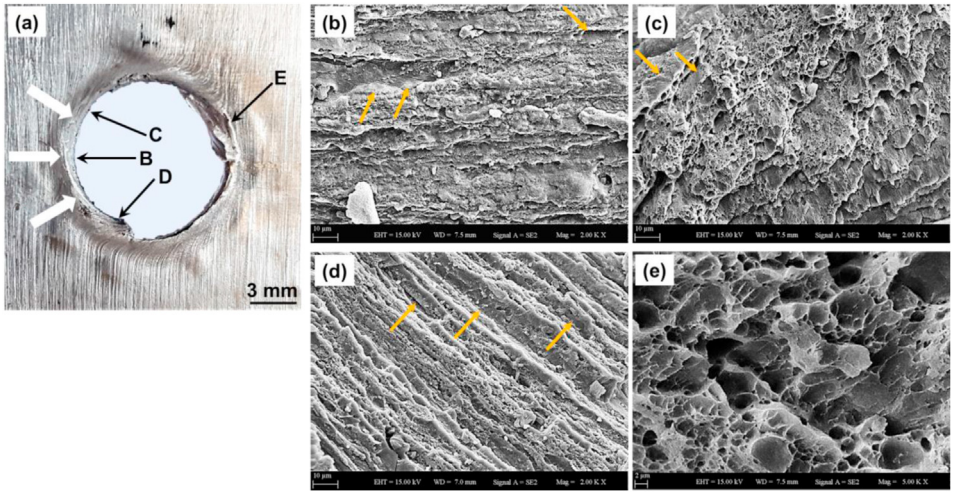


Fig. 14 – Fracture surface images on the upper sheet of T6 welds, bottom surface: (a) $L_{max} = 500$ N and $N_f = 1.44 \times 10^6$ and (b–e) magnified views at points B-E in (a), respectively. The loading direction is horizontal.

respectively. It is clear that B, C, and D regions indicate striated fracture patterns (marked by arrows), whereas point E displays a crack surface with a well-defined geometry similar to static fracture [44,46,47]. The crack initiated at the boundary between the upper sheet and lower sheet and propagated through the base metals. Based on Fig. 13a, it can also be noted that during fatigue, cracks grow from point B to E with increasing number of loading cycles. As such, it can be argued that crack initiated at the IL boundary and propagated in two directions, in the upper sheet around the weld nugget and in the lower sheet longitudinal along the loading direction (Fig. 10d) before complete fracture of the joint, leaving most of the nugget within the lower sheet.

The fracture surface observations at the lowest load level for T6 temper joints is shown in Fig. 14, where the regions indicated by arrows B-E are provided in Fig. 14b through Fig. 14e. Similar to the O temper joint, B, C, and D regions contain striation like patterns, while dimples are recognized around region E. The presence of striations spread in several directions can be attributed to the local changes in stress state around the nugget zone [44,48]. This suggests that the crack initiated at the boundary between the upper and lower sheets near to the nugget edge, and propagated along the perimeter of the nugget as shown by the arrows in Fig. 14a.

Based on the macroscopic and microscopic fracture surface observations, it can be asserted that fatigue failure takes place by crack propagation mainly along two paths, one at the lower sheet originating at the nugget perpendicular to the loading direction, and the other is at the upper sheet through the HAZ/TMAZ of the weld. Regarding the heat treatment effect, there is not any noticeable difference in the fracture mechanisms.

4. Conclusions

In the current work, intermediate layer friction stir spot welding (IL-FSSW) process is employed to join a pair of 6061 aluminum alloy sheets in annealed (O) and artificial aged (T6) heat treatment conditions. The results of the tensile and fatigue experiments were evaluated with the following conclusions:

1. Flat welds without keyhole formation were achieved in joining of 6061 aluminum alloys using the IL-FSSW process.
2. With the IL-FSSW process, it was possible to achieve decent levels of lap shear joint strengths exceeding those obtained by conventional and alternative techniques.
3. Under shear-tensile loading, the welds fractured in shear-plug mode for O temper joints and in plug mode for T6 temper joints. For both tempers, cyclic loading led to plug and shear-plug fracture under high and low stress regime, respectively.
4. Artificial aging had a positive effect on the fatigue life under high levels of cyclic loading, however there was not a distinct effect at lower loads. Specifically, joints of both tempers exhibited similar response at a load level of 500 N.

Declaration of Competing Interest

The authors declare that they have no known competing financial interests or personal relationships that could have appeared to influence the work reported in this paper.

Acknowledgements

Partial support from Ozyegin University research fund is acknowledged.

REFERENCES

[1] Agarwal H, Gokhale AM, Graham S, Horstemeyer MF. Void growth in 6061-aluminum alloy under triaxial stress state. Mater Sci Eng 2003;341:35–42.
[2] Ambriz RR, Mesmacque G, Ruiz A, Amrouche A, López VH, Benseddiq N. Fatigue crack growth under a constant amplitude loading of Al-6061-T6 welds obtained by modified indirect electric arc technique. Sci Technol Weld Join 2010;15:514–21.
[3] Uematsu Y, Tokaji K, Tozaki Y, Kurita T, Murata S. Effect of re-filling probe hole on tensile failure and fatigue behaviour of friction stir spot welded joints in Al–Mg–Si alloy. Int J Fatig 2008;30:1956–66.
[4] Thomas WM, Nicholas ED, Needhan JC, Murch MG, Temple-Smith P, Dawes CJ. International patent application PCT/GB92/02203 and GB patent application 9125978.8, vol. 6. London: UK Pat. Off; 1991.
[5] Dawes CJ, Thomas WM. Friction stir process welds aluminum alloys. Weld J 1996;75:41–51.
[6] Zhang Z, Yang X, Zhang J, Zhou G, Xu X, Zou B. Effect of welding parameters on microstructure and mechanical properties of friction stir spot welded 5052 aluminum alloy. Mater Des 2011;32:4461–70.
[7] Media Release. Mazda develops world's first aluminum joining technology using friction heat. 2003. www.mazda.com/publicity/release/0227e.html.
[8] Sun YF, Fujii H, Takaki N, Okitsu Y. Microstructure and mechanical properties of mild steel joints prepared by a flat friction stir spot welding technique. Mater Des 2012;37:384–92.
[9] Khan MI, Kuntz ML, Su P, Gerlich A, North T, Zhou Y. Resistance and friction stir spot welding of DP600: a comparative study. Sci Technol Weld Join 2007;12:175–82.
[10] Sun YF, Fujii H, Takaki N, Okitsu Y. Novel spot friction stir welding of 6061 and 5052 Al alloys. Sci Technol Weld Join 2011;16:605–12. https://doi.org/10.1179/1362171811Y.0000000043.
[11] Shen Z, Ding Y, Gopkalo O, Diak B, Gerlich AP. Effects of tool design on the microstructure and mechanical properties of refill friction stir spot welding of dissimilar Al alloys. J Mater Process Technol 2018;252:751–9. https://doi.org/10.1016/j.jmatprotec.2017.10.034.
[12] Shahrabadi AR, Mousavizade SM, Ezatpour HR, Pouranvari M. Achieving high mechanical performance in protrusion friction stir spot welding (PFSSW) of DQSK steel compared to other techniques. Mater Res Express 2018;5:106519.
[13] Fujimoto M, Inuzuka M, Koga S, Seta Y. Development of friction spot joining. Weld World 2005;49:18–21.

[14] Arici A, Mert Ş. Friction stir spot welding of polypropylene. J Reinforc Plast Compos 2008;27:2001–4.
[15] Itapu SK, Muci-Küchler KH. Visualization of material flow in the refill friction stir spot welding process. SAE Technical Paper. 2006.
[16] Gao C, Gao R, Ma Y. Microstructure and mechanical properties of friction spot welding aluminium–lithium 2A97 alloy. Mater Des 2015;83:719–27.
[17] Lathabai S, Painter MJ, Cantin GMD, Tyagi VK. Friction spot joining of an extruded Al–Mg–Si alloy. Scripta Mater 2006;55:899–902.
[18] Gerlich A, Yamamoto M, North TH. Strain rates and grain growth in Al 5754 and Al 6061 friction stir spot welds. Metall Mater Trans 2007;38:1291–302.
[19] Shen Z, Yang X, Yang S, Zhang Z, Yin Y. Microstructure and mechanical properties of friction spot welded 6061-T4 aluminum alloy. Mater Des 2014;54:766–78.
[20] Zhou L, Liu D, Nakata K, Tsumura T, Fujii H, Ikeuchi K, et al. New technique of self-refilling friction stir welding to repair keyhole. Sci Technol Weld Join 2012;17:649–55.
[21] Lin P-C, Su Z-M, He R-Y, Lin Z-L. Failure modes and fatigue life estimations of spot friction welds in cross-tension specimens of aluminum 6061-T6 sheets. Int J Fatig 2012;38:25–35.
[22] Hassanifard S, Mohammadpour M, Rashid HA. A novel method for improving fatigue life of friction stir spot welded joints using localized plasticity. Mater Des 2014;53:962–71.
[23] American Welding Socity (Aws). Specification for automotive weld quality- resistance spot welding of steel. 2007.
[24] Ibrahim IJ, Yapici GG. Effect of processing parameters on the strength of keyhole free friction stir spot aluminum welds. In: AIP conf. Proc. AIP Publishing LLC; 2019. p. 20020.
[25] Ibrahim IJ, Yapici GG. Application of a novel friction stir spot welding process on dissimilar aluminum joints. J Manuf Process 2018;35:282–8.
[26] Ibrahim IJ, Yapici GG. Optimization of the intermediate layer friction stir spot welding process. Int J Adv Manuf Technol 2019;104:993–1004.
[27] A S M H. Metallography and microstructuresVol, 9. Park. OH: ASM Int. Mater; 2004.
[28] Wiedenhoft AG, de Amorim HJ, de Rosendo TS, Tier MAD, Reguly A. Effect of heat input on the mechanical behaviour of Al-Cu FSW lap joints. Mater Res 2018;21.
[29] Kubit A, Bucior M, Wydrzyński D, Trzepieciński T, Pytel M. Failure mechanisms of refill friction stir spot welded 7075-T6 aluminium alloy single-lap joints. Int J Adv Manuf Technol 2018;94:4479–91.
[30] Tozaki Y, Uematsu Y, Tokaji K. Effect of processing parameters on static strength of dissimilar friction stir spot welds between different aluminium alloys. Fatig Fract Eng Mater Struct 2007;30:143–8.
[31] Tozaki Y, Uematsu Y, Tokaji K. Effect of tool geometry on microstructure and static strength in friction stir spot welded aluminium alloys. Int J Mach Tool Manufact 2007;47:2230–6. https://doi.org/10.1016/j.ijmachtools.2007.07.005.
[32] Lin P-C, Pan J, Pan T. Failure modes and fatigue life estimations of spot friction welds in lap-shear specimens of aluminum 6111-T4 sheets. Part 2: welds made by a flat tool. Int J Fatig 2008;30:90–105.
[33] Rosendo T, Parra B, Tier MAD, da Silva AAM, dos Santos JF, Strohaecker TR, et al. Mechanical and microstructural investigation of friction spot welded AA6181-T4 aluminium alloy. Mater Des 2011;32:1094–100. https://doi.org/10.1016/j.matdes.2010.11.017.
[34] Fujimoto M, Koga S, Abe N, Sato YS, Kokawa H. Microstructural analysis of stir zone of Al alloy produced by friction stir spot welding. Sci Technol Weld Join 2008;13:663–70. https://doi.org/10.1179/136217108x347601.
[35] Garg A, Bhattacharya A. Strength and failure analysis of similar and dissimilar friction stir spot welds: influence of different tools and pin geometries. Mater Des 2017;127:272–86. https://doi.org/10.1016/j.matdes.2017.04.084.
[36] Jeon CS, Hong ST, Kwon YJ, Cho HH, Han HN. Material properties of friction stir spot welded joints of dissimilar aluminum alloys. Trans. Nonferrous Met. Soc. China (English Ed. 2012;22:s605–13. https://doi.org/10.1016/S1003-6326(12)61772-5.
[37] Bakavos D, Chen Y, Babout L, Prangnell P. Material interactions in a novel pinless tool approach to friction stir spot welding thin aluminum sheet. Metall. Mater. Trans. A Phys. Metall. Mater. Sci. 2011;42:1266–82. https://doi.org/10.1007/s11661-010-0514-x.
[38] Uematsu Y, Tokaji K, Murata S, Tozaki Y, Kurita T. Fatigue behaviour of friction stir spot welded Al-Mg-Si alloy. J. Soc. Mater. Sci. Japan. 2007;56:537–43. https://doi.org/10.2472/jsms.56.537.
[39] Uematsu Y, Tokaji K, Tozaki Y, Kurita T, Murata S. Effect of post-heat treatment on the fatigue behaviour of a friction stir spot-welded Al–Mg–Si alloy. Weld Int 2009;23:481–9.
[40] Chowdhury SH, Chen DL, Bhole SD, Cao X, Wanjara P. Lap shear strength and fatigue behavior of friction stir spot welded dissimilar magnesium-to-aluminum joints with adhesive. Mater Sci Eng 2013;562:53–60. https://doi.org/10.1016/j.msea.2012.11.039.
[41] Chowdhury SH, Chen DL, Bhole SD, Cao X, Wanjara P. Lap shear strength and fatigue life of friction stir spot welded AZ31 magnesium and 5754 aluminum alloys. Mater Sci Eng 2012;556:500–9. https://doi.org/10.1016/j.msea.2012.07.019.
[42] Lin P-C, Pan J, Pan T. Failure modes and fatigue life estimations of spot friction welds in lap-shear specimens of aluminum 6111-T4 sheets. Part 1: welds made by a concave tool. Int J Fatig 2008;30:74–89. https://doi.org/10.1016/j.ijfatigue.2007.02.016.
[43] Venukumar S, Muthukumaran S, Yalagi SG, V Kailas S. Failure modes and fatigue behavior of conventional and refilled friction stir spot welds in AA 6061-T6 sheets. Int J Fatig 2014;61:93–100.
[44] Venukumar S, Yalagi SG, Muthukumaran S, V Kailas S. Static shear strength and fatigue life of refill friction stir spot welded AA 6061-T6 sheets. Sci Technol Weld Join 2014;19:214–23.
[45] Li Z, Ji S, Ma Y, Chai P, Yue Y, Gao S. Fracture mechanism of refill friction stir spot-welded 2024-T4 aluminum alloy. Int J Adv Manuf Technol 2016;86:1925–32.
[46] Uematsu Y, Kakiuchi T, Tozaki Y. Fatigue behavior of dissimilar friction stir spot welds between A6061 and AZ31 fabricated by a scroll grooved tool without probe. In: Fujii W, editor. H.B.T.-P. of the 1st I.J.S. on J. Woodhead Publishing; 2013. p. 213–8. https://doi.org/10.1533/978-1-78242-164-1.213.
[47] Murakami Y. 15 - the mechanism of fatigue failure in the very high cycle fatigue (VHCF) life regime of N> 107 cycles. In: Murakami E, editor. Y.B.T.-M.F. Academic Press; 2019. p. 341–406. https://doi.org/10.1016/B978-0-12-813876-2.00015-7.
[48] Brzostek RC. Damage tolerance of refill Friction Stir Spot Weld application for the aircraft industry. 2019.